THE JOURNAL OF BIOLOGICAL CHEMISTRY VOL. 280, NO. 51, pp. 42325–42335, December 23, 2005

Regulated Localization of Rab18 to Lipid Droplets

EFFECTS OF LIPOLYTIC STIMULATION AND INHIBITION OF LIPID DROPLET CATABOLISM[*][S]

Received for publication, June 20, 2005, and in revised form, September 15, 2005 Published, JBC Papers in Press, October 5, 2005, DOI 10.1074/jbc.M506651200

Sally Martin[‡1], **Kim Driessen**[‡], **Susan J. Nixon**[‡], **Marino Zerial**[§], **and Robert G. Parton**[‡]

From the [‡]*Institute for Molecular Bioscience & Centre for Microscopy and Microanalysis, University of Queensland, Brisbane, Queensland 4072, Australia and the* [§]*Max Planck Institute for Molecular Cell Biology and Genetics, Pfotenhauerstrasse 108, 01307 Dresden, Germany*

Rab GTPases are crucial regulators of membrane traffic. Here we have examined a possible association of Rab proteins with lipid droplets (LDs), neutral lipid-containing organelles surrounded by a phospholipid monolayer, also known as lipid bodies, which have been traditionally considered relatively inert storage organelles. Although we found close apposition between LDs and endosomal compartments labeled by expressed Rab5, Rab7, or Rab11 constructs, there was no detectable labeling of the LD surface itself by these Rab proteins. In contrast, GFP-Rab18 localized to LDs and immunoelectron microscopy showed direct association with the monolayer surface. Green fluorescent protein (GFP)-Rab18-labeled LDs underwent oscillatory movements in a localized area as well as sporadic, rapid, saltatory movements both in the periphery of the cell and toward the perinuclear region. In both adipocytes and non-adipocyte cell lines Rab18 localized to a subset of LDs. To gain insights into this specific localization, Rab18 was co-expressed with Cav3^{DGV}, a truncation mutant of caveolin-3 shown to inhibit the catabolism and motility of lipid droplets. GFP-Rab18 and mRFP-Cav3^{DGV} labeled mutually exclusive subpopulations of LDs. Moreover, in 3T3-L1 adipocytes, stimulation of lipolysis increased the localization of Rab18 to LDs, an effect reversed by β-adrenergic antagonists. These results show that a Rab protein localizes directly to the monolayer surface of LDs. In addition, association with the LD surface was increased following stimulation of lipolysis and inhibited by a caveolin mutant suggesting that recruitment of Rab18 is regulated by the metabolic state of individual LDs.

The maintenance of lipid homeostasis within the cell is controlled through combined synthesis, influx, efflux, and storage. Cells store excess fatty acids and cholesterol in lipid droplets (LDs),[2] which are dynamic and regulated organelles derived from the endoplasmic reticulum (ER) (1, 2). LDs have been shown to undergo microtubule-based motility (3–5) and to interact with a range of other organelles, including mitochondria, peroxisomes, and the ER (6, 7). Whereas LDs have been best described in adipocytes and steroidogenic cells of the testis, ovary, and adrenal gland, they are also present in a range of other cell types, and their formation can be induced in cultured cells by oleic acid treatment (3), suggesting that all cells have the ability to generate LDs under conditions of elevated fatty acids. In recent years interest in the regulation of LDs in less specialized cell types has increased significantly, due in part to the observation that a dominant-negative truncation mutant of caveolin, Cav3^{DGV}, is localized to the surface of LDs and induces a cholesterol imbalance in fibroblasts, in addition to inhibiting LD motility and catabolism (3, 8). Caveolins have been shown to bind cholesterol (9) and fatty acids (10), and while predominantly localized to caveolar domains of the cell surface they can be redistributed to LDs upon fatty acid treatment (3). In addition to the inhibitory effects of Cav3^{DGV} on the LD, Cav3^{DGV} also indirectly inhibits signaling from the cell surface through an effect on cholesterol, suggesting a link between the function of the LDs and functional maintenance of cell surface domains.

To begin to define the mechanisms regulating the formation and catabolism of the LD it is important to first identify the nature of the interaction of this organelle with other compartments within the cell. Several recent studies have undertaken proteomic analyses of LDs from a number of different cell types, under conditions of lipolysis or lipid deposition. These analyses identified numerous members of the Rab family of small GTPases associated with the LDs (11–14). The Rab family of proteins are essential regulators of vesicular traffic. Described as molecular switches, Rab proteins undergo conformational changes through cycles of GTP binding and hydrolysis (15, 16). The GTP-bound active form interacts directly with downstream effectors and indirectly with other components of the transport machinery controlling cargo selection, vesicle fusion, cytoskeletal transport, and integration of vesicle traffic with signal transduction pathways. Although the novel nature of the LD hemi-membrane makes it unlikely that proteins spanning the bilayer could associate with this organelle, this would not preclude association of Rab proteins whose attachment to membranes is regulated through prenylation at the C terminus, and protein-protein interactions (15, 16). Indeed, ten Rab GTPases have been found associated with LDs (11–14), several of which have been previously localized to endocytic compartments. On the one hand, this complexity is not unusual, as several distinct Rab proteins can be associated with a single organelle undertaking multiple sorting functions, such as early endosomes and the Golgi complex (16). The predicted association of multiple Rab proteins with the lipid droplet suggests a dynamic interaction between this and other organelles in the cell. On the other hand, out of the Rab proteins associated with LDs, only five, *i.e.* Rab5c, Rab7, Rab10, Rab14, and Rab18, have been identified independently in at least two separate studies.

In the present study we have analyzed the localization of Rab5, Rab7, Rab11, and Rab18, all previously identified in the endosomal system,

* This work was supported by a grant from the National Health and Medical Research Council of Australia (to R. G. P.). Confocal microscopy was performed at the Australian Cancer Research Foundation (ACRF)/Institute for Molecular Bioscience (IMB) Dynamic Imaging Facility for Cancer Biology, established with funding from the ACRF. Electron microscopy was performed at the Centre for Microscopy and Microanalysis at the University of Queensland. The IMB is a Special Research Centre of the Australian Research Council. The costs of publication of this article were defrayed in part by the payment of page charges. This article must therefore be hereby marked "*advertisement*" in accordance with 18 U.S.C. Section 1734 solely to indicate this fact.

[S] The on-line version of this article (available at http://www.jbc.org) contains supplemental videos 1–5.

[1] To whom correspondence should be addressed. Tel.: 61-7-3346-2030; Fax: 61-7-3346-2101; E-mail: s.martin@imb.uq.edu.au.

[2] The abbreviations used are: LD, lipid droplet; ER, endoplasmic reticulum; TVE, tubulovesicular elements; PFA, paraformaldehyde; BHK, baby hamster kidney cells; BSA, bovine serum albumin; GFP, green fluorescent protein; YFP, yellow fluorescent protein; MRFP, monomeric red fluorescent protein; PIPES, 1,4-piperazinediethanesulfonic acid.

with respect to LDs under conditions of neutral lipid synthesis. We have identified Rab18 as a major component of lipid droplets and further explored its role in lipid dynamics and lipid storage activities.

MATERIALS AND METHODS

Cell Culture—3T3-L1 fibroblasts (American Type Culture Collection, Rockville, MD) were maintained in Dulbecco's modified Eagle's medium supplemented with 10% fetal calf serum and 2 mM L-glutamine, and differentiated using insulin, dexamethasone, biotin, and isobutylmethylxanthine as described previously (17). Adipocytes were used between days 6 and 12 post-differentiation, or at 2-day intervals during the differentiation process as described in the results section. BHK-21 cells (baby hamster kidney cells) and Vero cells (African green monkey kidney epithelial cells) were maintained in Dulbecco's modified Eagle's medium supplemented with 10% (v/v) Serum-Supreme (BioWhittaker) and 2 mM L-glutamine.

Antibodies, Plasmids, and Reagents—Mouse anti-GM130 (catalog no. 610823), monoclonal anti-caveolin-1 (catalog no. 610406), and monoclonal anti-caveolin-2 (catalog no. 610684) were obtained from BD Transduction Laboratories (BD Biosciences). Rabbit anti-perilipin A (catalog no. P1998) and mouse anti-α-tubulin (catalog no. T9026) were obtained from Sigma. Rabbit anti-Rab18 (18) and rabbit anti-GFP (19) have been described previously. Alexa488- and Alexa594-conjugated secondary antibodies were obtained from Molecular Probes Inc. (Eugene, OR). Horseradish peroxidase-conjugated secondary antibodies were obtained from Sigma. Oleic acid was obtained from Calbiochem and conjugated to fatty-acid free bovine serum albumin (Calbiochem) prior to use. Bodipy493/503 and Nile Red were obtained from Molecular Probes and prepared as saturated solutions in ethanol (working dilution, 1:200) and acetone (working dilution, 1:2000), respectively. All other chemicals were obtained from Sigma unless stated otherwise.

GFP-Rab5 and YFP-Rab11 have been described previously (20). GFP-Rab7 was obtained from Dr. Lucas Pelkmans, Max-Planck Institute, Dresden, Germany. mRFP-Cav3^{DGV} was constructed using Cav3^{DGV}-HA (21) as a template to amplify a fragment using the following primers: 5′-GGGGTACCCGACGGTGTATGGAAGGTG-3′ and 5′-CGGGATCCTAGCCTTCCCTTCGCAG-3′. The PCR product was A-tailed and cloned into pGEM-T Easy (Promega, Madison, WI) and subsequently excised using BamHI and KpnI, and ligated into linearized mRFP-C3. mRFP-C3 was constructed from pRSETb-mRFP1 (supplied by Prof. Roger Tsien, Howard Hughes Medical Institute, University of California (22)).

To generate GFP-Rab18, the mouse Rab18 ORF was excised from myc-Rab18 using NdeI and BamHI (removing the myc tag), ligated into pSL1180 (Amersham Biosciences), and subsequently excised with BamHI and PstI and ligated into pEGFP-C1 (Clontech), resulting in an N-terminal GFP tag. All constructs were sequenced using ABI PRISM BigDye Terminator version 3.1 (Applied Biosystems, Foster City, CA) in the Australian Genome Research Facility, University of Queensland.

Indirect Immunofluorescence Microscopy and Real-time Video Microscopy—For immunofluorescence microscopy cells grown on glass coverslips were fixed with 4% paraformaldehyde (PFA) in PBS. Cells were permeabilized in 0.1% saponin (w/v) for 10 min, quenched for 10 min using 50 mM $NHCl_4$, and blocked for 10 min using 0.2% bovine serum albumin/0.2% fish skin gelatin in PBS. Primary and secondary antibodies were diluted in blocking solution and incubated with the cells for 30 min at room temperature. Finally the coverslips were washed in PBS and mounted in Mowiol (Calbiochem). Labeling was analyzed using an Axiovert 200M SP LSM 510 META confocal laser scanning microscope (Zeiss) under oil, using either 100× or 63× oil immersion objectives. The data were processed using the LSM 510 Meta (Zeiss) software, and images were assembled using Photoshop 7.0 (Adobe Systems, Mountain View, CA). Quantitation of LD Rab18 labeling was performed on fluorescence images collected with identical settings, using ImageJ 1.33 to measure the mean pixel intensity of individual LDs. For each individual experiment between 20 and 70 LDs were analyzed.

Cells for real-time microscopy were plated onto glass-bottom tissue culture dishes (MatTek Corp.) and transferred into CO_2-independent medium supplemented with 0.1% fatty-acid free bovine serum albumin (Calbiochem) in the presence or absence of 100 μg/ml oleic acid. Time series were collected at 37 °C using an Axiovert 200M SP LSM 510 Meta confocal laser scanning microscope equipped with a heated stage and a 100× oil immersion objective. Cells were used for real-time data collection for a maximum of 1.5 h. Time series images were collected using a 488 nm excitation laser line at <20% maximum power using the Zeiss LSM510 Meta software. Images were converted to 8-bit TIFF files and further analyzed using ImageJ software (National Institutes of Health, Bethesda, MD). QuickTime movies were assembled using ImageJ 1.33, and still images were compiled using Adobe Photoshop 7.0.

LD Isolation—LDs were isolated using a modification of the procedure of Yu *et al.* (23). Briefly, cells were scraped into dissociation buffer (25 mM Tris-HCl, pH 7.4, 100 mM KCl, 1 mM EDTA, 5 mM EGTA) containing a mixture of protease inhibitors (250 μM phenylmethylsulfonyl fluoride, 10 μg/ml aprotinin, and 10 μg/ml leupeptin), and lysed by sonication for 10 s. LDs were isolated by sucrose density gradient centrifugation through 18.5%, 9%, and 4.1% sucrose steps and through top buffer (25 mM Tris-HCl, pH 7.4, 1 mM EDTA, 1 mM EGTA). Gradients were analyzed by Western blotting or by electron microscopy.

Immunoprecipitation and Western Blotting—Immunoprecipitation was carried out essentially as described previously (24). Briefly, cells were lysed in 50 mM Tris, pH 7.4, 150 mM NaCl, 5 mM EDTA containing 1% Nonidet P-40, 0.1% SDS, and protease inhibitors. Equal volumes of lysates were immunoprecipitated using either Rab18 antiserum, GFP antiserum, or a non-immune rabbit serum and collected using protein A-Sepharose beads. Immunoprecipitated proteins were solubilized directly into Laemmli sample buffer and analyzed by SDS-PAGE and Western blotting as described previously (25). Immunolabeled proteins were visualized using horseradish peroxidase-conjugated secondary antibodies and developed using the Supersignal ECL reagent (Pierce).

Electron Microscopy—Immunoelectron microscopy of ultrathin cryosections was performed essentially as described previously (26, 27). Briefly, Vero cells transfected with GFP-Rab18 were incubated overnight in the presence of 100 μg/ml oleic acid and fixed in 2% paraformaldehyde/0.2% glutaraldehyde in 0.1 M PHEM buffer (60 mM PIPES, 25 mM HEPES, 2 mM $MgCl_2$, 10 mM EGTA), pH 6.9, for 1 h at room temperature. Cells were embedded in 10% gelatin, cryoprotected using PVP-sucrose, and snap frozen onto specimen holders in liquid N_2. Ultracryomicrotomy was performed by a slight modification of the Tokuyasu technique (28) as described previously (27), and sections were picked up with a 1:1 mixture of 2.3 M sucrose and 2% methyl cellulose (29). Grids were viewed using a Jeol 1010 transmission electron microscope.

To perform immunoelectron microscopy on isolated LDs, BHK cells were transfected with GFP-Rab18 or GFP and subsequently incubated in 100 μg/ml oleic acid overnight. LDs were isolated using sucrose density gradient centrifugation as described above, and the top fractions, containing the LDs, were fixed in 4% PFA. Isolated LDs were applied to Formvar/carbon-coated copper grids and immunolabeled as described previously (25).

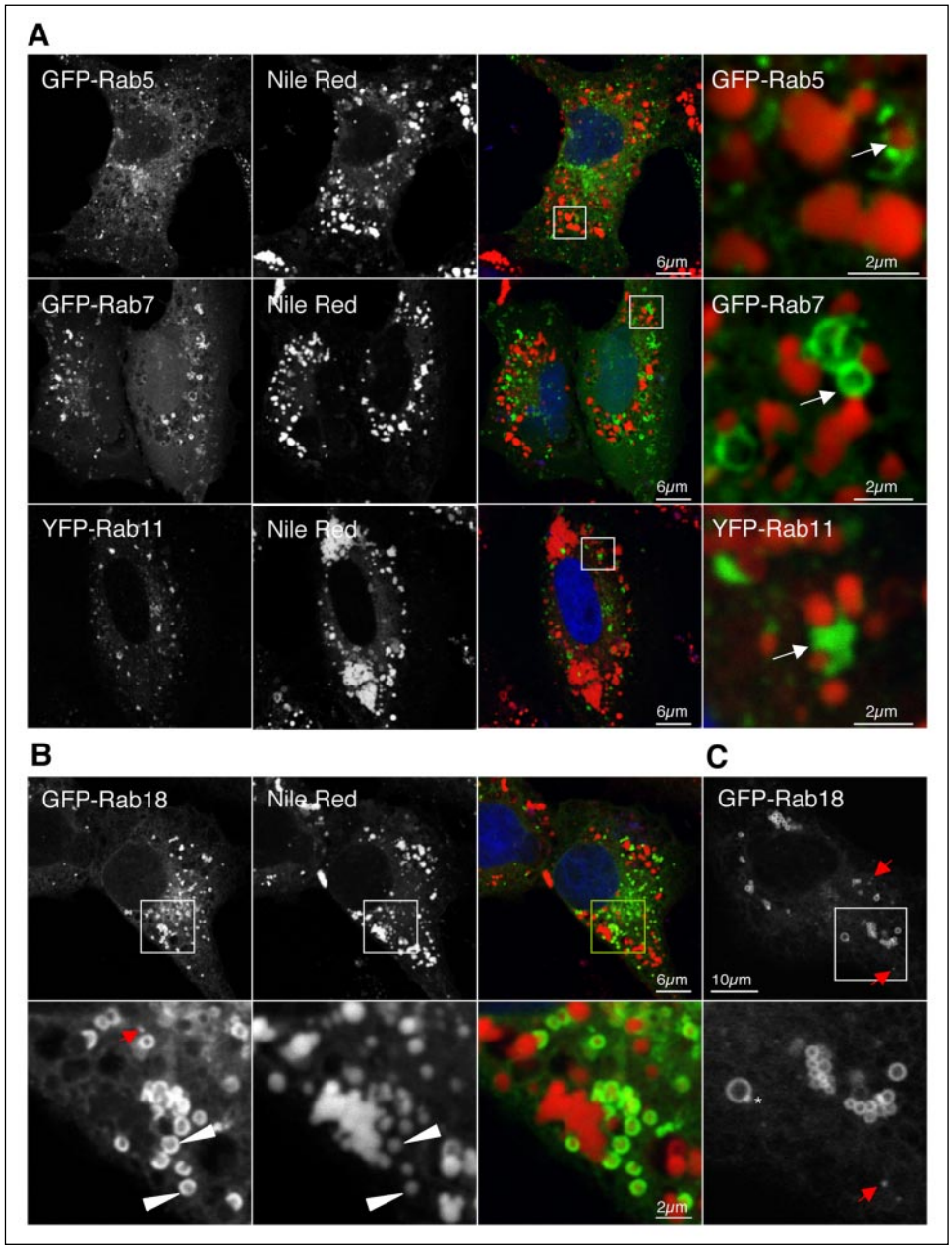

FIGURE 1. **Localization of GFP-Rab proteins in oleic acid-treated Vero cells.** Vero cells expressing fluorescently tagged Rab5, Rab7, Rab11, or Rab18 were incubated with 100 μg/ml oleic acid overnight, fixed in 4% PFA, and counterstained using Nile Red to identify LDs. *A*, a proportion of GFP-Rab5-, YFP-Rab11-, and GFP-Rab7-labeled endosomes were all observed in close proximity to LDs (*arrows*) but did not label the surface of the LD itself. *B*, GFP-Rab18 was identified in the ER, on the surface of a subset of LDs (*arrowheads*), and as small puncta distributed throughout the cell (*red arrows*). LD labeling was often crescent-shaped in fixed cells. *C*, Vero cells expressing GFP-tagged Rab18 were incubated in oleic acid overnight and imaged in real-time in the absence of fixation. In live cells GFP-Rab18 was observed in the reticular ER, as rings surrounding a subset of LDs and as small puncta (*red arrows*) distributed throughout the cell. A small bright punctate dot of Rab18 labeling was occasionally observed at the periphery of the labeled LDs (*asterisk*).

RESULTS

Localization of GFP-Rab18 to Lipid Droplets and Apposition of Endosomal Compartments—To investigate the localization of Rab GTPases potentially involved in LD function in relation to LDs we expressed fluorescently tagged Rab5, Rab7, Rab11, and Rab18 in Vero cells. To increase LD formation, cells were incubated overnight in 100 μg/ml oleic acid conjugated to bovine serum albumin. Fatty acid concentrations higher than physiological levels have been used previously to induce the rapid formation of LDs in cultured cells (3). Lower concentrations of oleic acid induced a similar formation over a longer period of time (results not shown). GFP-Rab5 and YFP-Rab11 were identified in punctate structures distributed throughout the cell (Fig. 1*A*) consistent with localization to early and recycling endosomes, respectively (20). In contrast, GFP-Rab7 was present in both small punctate vesicles and in larger endosomal vacuoles, consistent with localization to late endosomes (30). All isoforms also showed varying levels of a cytosolic pool, frequently observed when Rab proteins are over-expressed (31). When cells were counterstained with Nile Red to identify lipid droplets, both GFP-Rab5- and YFP-Rab11-containing structures were occasionally identified in close apposition to Nile Red-positive structures, whereas GFP-Rab7-labeled endosomes were frequently observed in close apposition to LDs (Fig. 1*A*). However, Rab5, Rab7, and Rab11 were not observed to label the LD surface itself. In contrast, GFP-Rab18 showed specific and intense labeling of a subset of LDs (Fig. 1, *B* and *C*). In addition, GFP-Rab18 labeled the ER and small, possibly ER-associated, puncta distributed throughout the cells, as well as weak labeling in the region of the Golgi complex (Figs. 1*B*, 1*C*, and 4). In a small number of cells with very high levels of GFP-Rab18 expression there was a very strong labeling of the perinuclear region, and in these cells labeling for the Golgi marker GM130 suggested that the Golgi complex was disrupted in a similar manner to brefeldin A (results not shown). However, the predominant localization of GFP-Rab18 was to the LDs. GFP-Rab18 consistently labeled smaller sized LDs usually at the periphery of larger, unlabeled LDs, or a cluster of LDs (Fig. 1*B*). Intriguingly, in fixed cells

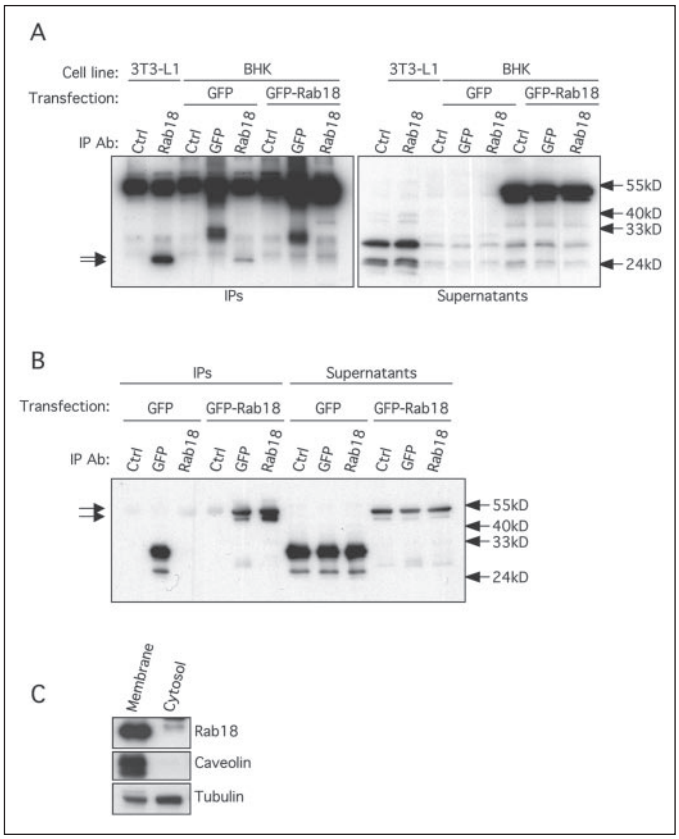

FIGURE 2. **Immunoprecipitation of endogenous and expressed Rab18.** *A* and *B*, immunoprecipitation of endogenous Rab18 and transfected GFP-Rab18 from 3T3-L1 adipocytes and BHK cells. Endogenous Rab18 was immunoprecipitated from solubilized 3T3-L1 adipocyte cell lysates using an antiserum raised against Rab18 or a control pre-immune rabbit serum (*Ctrl*). In addition, BHK cells were transfected with either GFP-Rab18 or GFP, and transfected proteins were immunoprecipitated using antisera raised against Rab18, GFP, or a pre-immune rabbit serum (*Ctrl*). Immunoprecipitations (*IPs*) and IP supernatants were analyzed by Western blotting using an anti-Rab18 antiserum (*A*) or an anti-GFP antibody (*B*). Rab18 antiserum was found to specifically immunoprecipitate a single protein of apparent molecular mass of 26 kDa from both GFP-transfected BHK cells and 3T3-L1 adipocytes, and a protein band of ~55 kDa from GFP-Rab18-transfected cells. Conversely, GFP antiserum was found to specifically immunoprecipitate GFP-Rab18, which could be detected using either the anti-GFP antiserum (*B*) or the anti-Rab18 antiserum (*A*). Both transfected Rab18 and endogenous Rab18 resolved as a doublet (*arrows*) in the supernatants. A second protein band of ~31 kDa was also consistently recognized by the Rab18 antiserum in the supernatants but was not immunoprecipitated by the antibody. *C*, endogenous Rab18 is predominantly membrane associated. 3T3-L1 adipocyte cell lysates were fractionated into membrane and cytosol by ultracentrifugation. Proteins (10 μg) were analyzed by SDS-PAGE and Western blotting for endogenous Rab18, caveolin, and α-tubulin. Rab18 and caveolin were predominantly membrane-associated, whereas tubulin displayed both membrane-associated and cytosolic pools.

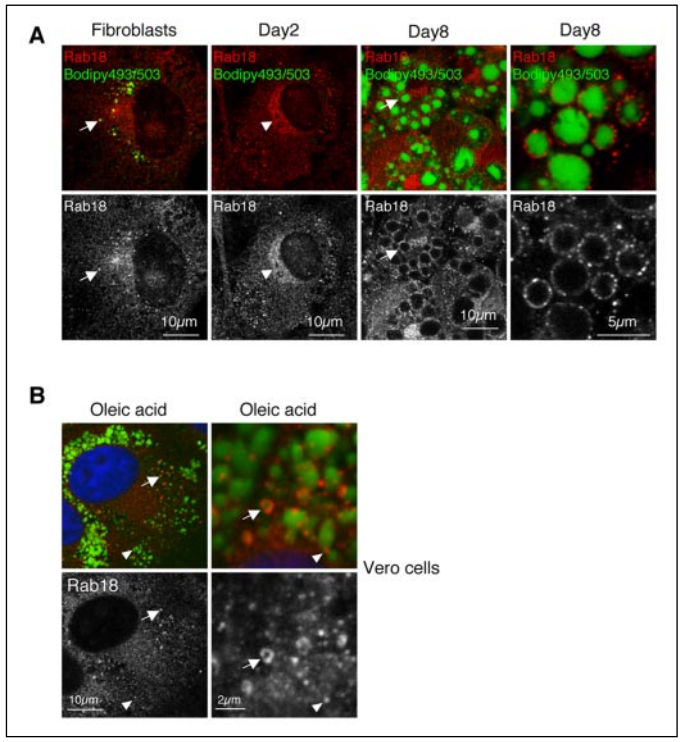

FIGURE 3. **Endogenous Rab18 localizes to LDs in fibroblasts and adipocytes, but is not up-regulated during differentiation.** *A*, 3T3-L1 fibroblasts were differentiated into adipocytes, fixed at various time points during the differentiation process, and labeled for Rab18. LDs were detected using Bodipy493/503. Rab18 was observed to label the surface of LDs in both fibroblasts and adipocytes (*arrows*). During the differentiation there was an increase in Golgi labeling (*arrowheads*). In fully differentiated adipocytes, Rab18 labeling was observed in distinct domains over the LD surface. *B*, Vero cells were treated overnight with 100 μg/ml oleic acid and fixed for immunofluorescence microscopy. Fixed cells were labeled for Rab18 and counterstained using Bodipy493/503 to label LDs, and 4′,6-diamidino-2-phenylindole to label the nucleus. Following treatment with oleic acid Rab18 was observed to label the surface of a subset of LDs, either as a ring shape (*arrows*) or as a single punctate dot (*arrowheads*).

GFP-Rab18 labeling was often observed to partially surround a LD, forming a crescent-shaped profile by fluorescence microscopy, suggestive of a partial enfolding of the LD surface by the Rab18 compartment (*arrowheads*, Fig. 1*B*). However, when live cells were imaged in real-time (Fig. 1*C*), the GFP-Rab18 profile was invariably ring-shaped, suggesting that PFA fixation altered the surface structure of the LDs. Differences between LD size between live and fixed, labeled cells have been described previously (4). Interestingly, an additional observation in live cells, not detectable in fixed cells, was the presence of a single persistent brighter spot of Rab18 labeling occasionally observed on the LD surface, reminiscent of GFP-Rab5 on endosomal membranes (32) (Fig. 1*C*).

Localization of Endogenous Rab18 in Fibroblasts and Adipocytes—Although expressed GFP-Rab18, but not other tested Rab proteins, was clearly localized to LDs, we next sought to investigate the localization of the endogenous Rab18 protein, both in fibroblasts and in 3T3-L1 adipocytes, cells with a large number of active lipid droplets. A rabbit antiserum raised against Rab18 (18) was found to immunoprecipitate endogenous Rab18 and heterologously expressed GFP-Rab18 (Fig. 2, *A* and *B*), and to detect heterologously expressed GFP-Rab18 by immunofluorescence microscopy (results not shown). In addition, anti-Rab18 antiserum detected GFP-Rab18 immunoprecipitated using an antiserum raised against GFP. Both endogenous Rab18 and heterologously expressed GFP-Rab18 often resolved as a doublet by Western blotting, presumably corresponding to both prenylated and non-prenylated forms. Fractionation of 3T3-L1 adipocyte cell lysates into membrane and cytosol fractions demonstrated that at steady state Rab18 was predominantly membrane associated (Fig. 2*C*).

Expression of Rab18 was found to be higher in 3T3-L1 adipocyte lysates than in BHK or Vero cells by Western blotting (results not shown). We therefore hypothesized that expression could be directly related to LD formation. However, no change in expression of Rab18 was observed during differentiation of 3T3-L1 fibroblasts into adipocytes (results not shown). We next examined the localization of endogenous Rab18 in 3T3-L1 cells during differentiation to adipocytes. In 3T3-L1 fibroblasts, Rab18 labeling was only clearly detectable in a subset of cells containing endogenous LDs, where it was observed to localize to the LD surface (Fig. 3*A*). In addition, there was a low, dispersed, punctate labeling, not observed with a nonspecific anti-serum. During the differentiation process a more pronounced perinuclear labeling was detectable consistent with Golgi localization (Fig. 3*A*). Conversion of

3T3-L1 fibroblasts to an adipocyte phenotype, characterized by the accumulation of large amounts of neutral lipid, coincided with the localization of endogenous Rab18 to the LD surface. Rab18 was observed to label LDs with a distinct, punctate labeling pattern (Fig. 3*A*). A similar labeling pattern was observed in oleic acid-treated Vero cells, in which a small subset of LDs were labeled heavily for Rab18, whereas a large number of LDs had a single punctate dot of Rab18 labeling associated with the surface (Fig. 3*A*). Thus in both adipocytes and non-adipocyte cell lines endogenous Rab18 associates with a distinct subset of LDs. Rather than a spectrum of different labeling densities on different LDs, distinct LDs are either very strongly labeled or show negligible labeling.

In conclusion, Rab18 was the only Rab protein that appeared to show specific localization to the surface of LDs as judged by light microscopy. Whether this represented *bona fide* labeling of LDs was further investigated by immunoelectron microscopy.

GFP-Rab18 Associates with the ER and Discrete Subdomains of the LD Surface—We examined the distribution of GFP-Rab18 expressed in Vero cells treated with oleic acid overnight, by immunoelectron microscopy on frozen sections. In ultrathin cryosections (~60 nm thick) in which the membrane compartments of the cell could be clearly discerned, LDs were not well preserved, appearing as irregularly shaped electron-lucent structures (Fig. 4*A*). However, GFP-Rab18 labeling was clearly shown to decorate the surface of LDs. In addition, and consistent with the light microscopic observations, Rab18 labeled the ER and clusters of non-clathrin-coated tubulovesicular elements (TVE) both around the LD and distributed throughout the cell (Fig. 4, *A* and *B*). The localization of GFP-Rab18 to the ER was further examined by labeling for calnexin by immunofluorescence microscopy (Fig. 4, *D* and *E*). Calnexin labeling could be seen to surround, but not co-localize with, GFP-Rab18-labeled LDs (Fig. 4*E*). In the peripheral ER, calnexin and GFP-Rab18 showed a similar reticular pattern, but again there was no co-localization between the two proteins suggesting that they localize to distinct domains of the ER (Fig. 4*D*). The small clusters of GFP-Rab18-labeled TVE were observed as dense patches of labeling throughout the sections (Fig. 4*B*). The nature of these compartments is not yet known, but it is possible that they correspond to the small puncta observed by IF (Fig. 1, *B* and *C*) or disrupted Golgi elements in cells with a high expression of GFP-Rab18. To improve the morphological preservation of the LD surface, thicker cryosections (~100 nm) were also prepared and labeled for GFP-Rab18 (Fig. 4*C*). Although most membrane compartments were only poorly discernible in these sections, preservation of the LD surface and adjacent ER was improved. GFP-Rab18 was clearly observed to strongly label the outer layer of the LD, consistent with localization to the LD surface rather than the ER. In some LDs a thin single layer of membrane could be discerned between the ER membrane and the LD core (*arrows*, Fig. 4*B*, *inset*). We hypothesize that this corresponds to a region of the LD monolayer.

As there was very close apposition observed between the ER membranes and the LD surface (Fig. 4, *A–C*), we considered the resolution of labeling in the cryosections insufficient to determine whether Rab18 was associated with the monolayer proper or with associated membranes. To maximize GFP-Rab18 expression and localization to LDs, BHK cells were transfected with GFP-Rab18 or GFP, and a subcellular fraction was enriched in LDs isolated by flotation through a sucrose density gradient (Fig. 5*A*). The LD fractions were fixed directly in 4% PFA and applied to an EM grid. The fractions were then immunolabeled with anti-GFP antibodies followed by protein A-gold. Labeling for GFP-Rab18 was present over the entire LD surface in a heterogeneous pattern, with areas of high concentration containing electron dense networks (Fig. 5, *B–D*). Labeling was also observed to associate with membranous material associated with the LDs. In other areas GFP-Rab18 labeling was completely absent. These results show that GFP-Rab18 is associated with the LD surface monolayer, as well as associated membranes, and also suggest an association with distinct cytoplasmic domains of the LD surface. Specificity of the labeling was confirmed by the absence of labeling on GFP-Rab18 containing LDs using protein A-gold in the absence of the primary anti-GFP antibody (Fig. 5*E*) and by labeling LDs isolated from cells expressing GFP alone (Fig. 5*F*).

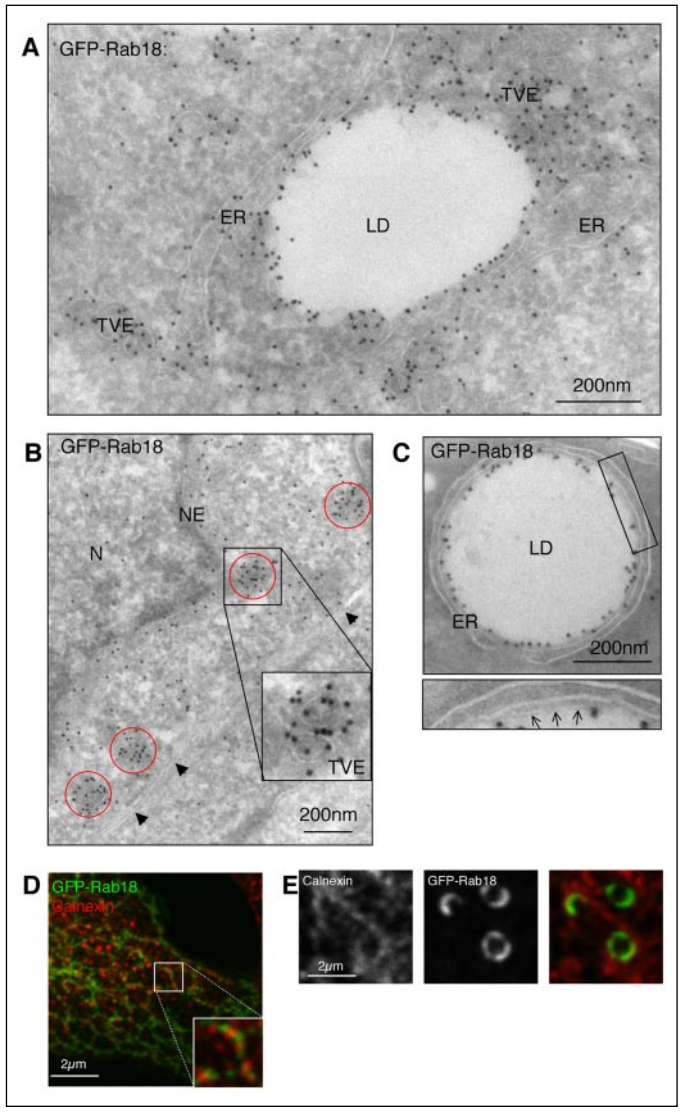

FIGURE 4. **Localization of GFP-Rab18 to LDs and the ER.** Vero cells expressing GFP-Rab18 were incubated with 100 μg/ml oleic acid overnight and fixed for immunoelectron microscopy (*A–C*) or immunofluorescence microscopy (*D* and *E*). For immunoelectron microscopy, cryosections were labeled using anti-GFP antibodies and labeling detected using 10 nm protein A-gold. LDs were defined as large, electron-lucent structures that lacked a limiting membrane bilayer. GFP-Rab18 was highly localized to the surface of LDs (*A* and *C*), to the peripheral ER (*A* and *D*) and nuclear envelope (*B*), as well as groups of small, non-clathrin-coated tubulovesicular elements (*TVE*) adjacent to the LD surface (*A*) and distributed throughout the cell (*B*). *C*, in thicker cryosections Rab18 labeled a thin membrane layer adjacent to the ER, assumed to correspond to the surface of the LD itself (*arrows*). Localization of GFP-Rab18 to the ER was confirmed by immunofluorescent microscopic labeling for calnexin (*D–E*). Calnexin-positive structures were seen surrounding the GFP-Rab18-labeled LDs (*D–E*), and in a punctate reticular pattern throughout the cell, contiguous with, but not co-localizing with, a punctate reticular GFP-Rab18 labeling pattern (*D*). Note that as fluorescence intensity of GFP-Rab18 at the LD surface was frequently much brighter than the surrounding ER, simultaneous visualization of the two localizations was impracticable. *ER*, endoplasmic reticulum; *LD*, lipid droplets; *NE*, nuclear envelope; *N*, nucleus; *TVE*, tubulovesicular elements; *arrowheads*, plasma membrane.

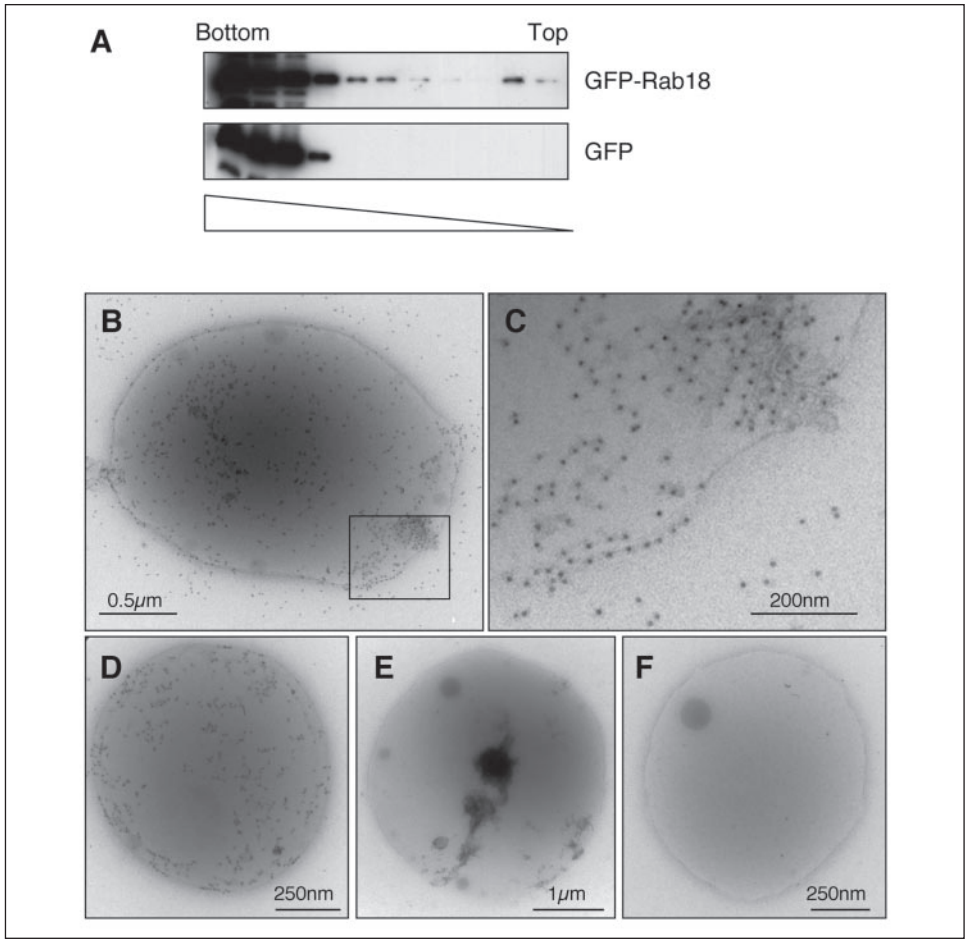

FIGURE 5. **Localization of GFP-Rab18 to the surface of isolated LDs.** To confirm the direct localization of GFP-Rab18 to the surface of the LDs, BHK cells were transfected with GFP-Rab18 (*A–E*) or GFP (*A* and *F*) and LDs isolated using sucrose density gradient centrifugation. *A*, a proportion of GFP-Rab18 was found to float in the top fractions of the sucrose gradient, corresponding to the LD fraction. *B–E*, isolated GFP-Rab18 LDs were mounted on EM grids and immunolabeled using an anti-GFP antibody followed by 10 nm protein A-gold (*B–D*), or by protein A-gold alone (*E*). GFP-Rab18 was found to label discrete patches over the surface of the LD, and membranous material associated with the LDs. Protein A-gold alone did not associate with the LDs. *F*, LDs isolated from cells expressing GFP alone were labeled using an anti-GFP antibody followed by 10 nm protein A-gold. The anti-GFP antibody did not label the surface of the LDs.

GFP-Rab18-labeled LDs and ER Compartments Are Highly Motile—Lipid droplets have been previously shown to undergo microtubule-based motility (3–5), which can be prevented by the depolymerization of microtubules (3, 4) or expression of the Cav3^{DGV} mutant (3). Inhibition of LD motility by Cav3^{DGV} suggests a role for motility in the functional regulation of LDs. To examine the motility of Rab18-labeled structures we expressed GFP-Rab18 in Vero cells that were subsequently treated with oleic acid overnight. Cells were imaged by real-time fluorescence microscopy in both the presence and absence of oleic acid to determine the motility of LDs and the ER under conditions of lipid deposition or catabolism. GFP-Rab18 was found to localize to both LDs (Fig. 6, *A* and *B*; supplementary data, videos 1 and 2) and the ER (Fig. 6, *C* and *E*; supplementary data, videos 3 and 5), as shown in Figs. 1–3, but in addition, smaller punctate and highly motile labeling was observed within the ER (Fig. 6*C*; supplementary data, video 4). All GFP-Rab18-labeled LDs underwent oscillatory movements and were seen to move in and out of the plane of focus within a given area of the cell (Fig. 6*A* (4)). However, a subset of GFP-Rab18-labeled LDs underwent rapid, saltatory movements, both in the periphery of the cell and to/from the microtubule organizing center. This was often observed to involve rapid movement in one direction, followed a few seconds later by a reverse motility back to the point of origin (Fig. 6, *A* and *B*). These linear, vectorial movements occurred over a period of 5 to 10 s and covered distances between 1 and 4 μm. The proportion of Rab18-labeled LDs undergoing saltatory rather than oscillatory movement (~6%) was unaffected by the presence of oleic acid. In addition to the movement of the LDs, there was also clear motility of the ER membranes themselves (Fig. 6*D*), as well as small puncta on the ER membrane (Fig. 6*C*), both of which underwent very rapidly motility in the periphery of the cells, and in close proximity to the LD membrane or to the cell surface. GFP-Rab18-labeled structures, presumed to be of ER origin, were also observed to extend away from groups of LDs (Fig. 6*E*). Together, these data clearly show that GFP-Rab18-labeled LDs are highly motile and display two distinct forms of motility, consistent with microtubule-based transient, vectorial movements of >1 μm, and shorter, tethered movements around a point of origin. Additionally, GFP-Rab18 confirms the highly dynamic nature of the ER system, displaying rapid motility throughout the cell and peripherally toward the cell surface.

GFP-Rab18 and mRFP-Cav3^{DGV} Localize to Distinct LD Populations—We have previously shown that an N-terminal truncation mutant of caveolin-3, Cav3^{DGV}, localizes to LDs and the ER and inhibits both the motility and the catabolism of LDs (3, 8). We hypothesized that the inhibition of LD catabolism by Cav3^{DGV} could be a direct result of an inhibition of the recruitment of Rab18 to these organelles. To simultaneously image both Cav3^{DGV} and Rab18, we generated an N-terminal mRFP-tagged Cav3^{DGV} construct. Localization of mRFP-Cav3^{DGV} was found to be identical to previously described YFP- and GFP-tagged constructs (8). mRFP-Cav3^{DGV} was localized to LDs and the ER and, following treatment with oleic acid, induced clumping of LDs in the perinuclear area (Fig. 7*A*). Furthermore, expression of mRFP-Cav3^{DGV} prevented the dispersal of LDs following recovery from oleic acid as described previously for YFP-tagged Cav3^{DGV} (3) (results not shown). Co-expression of mRFP-Cav3^{DGV} and GFP-Rab18 in Vero cells demonstrated that these two proteins co-localized within the ER, but localized to distinct subsets of LDs under normal growth conditions (Fig. 7*B*).

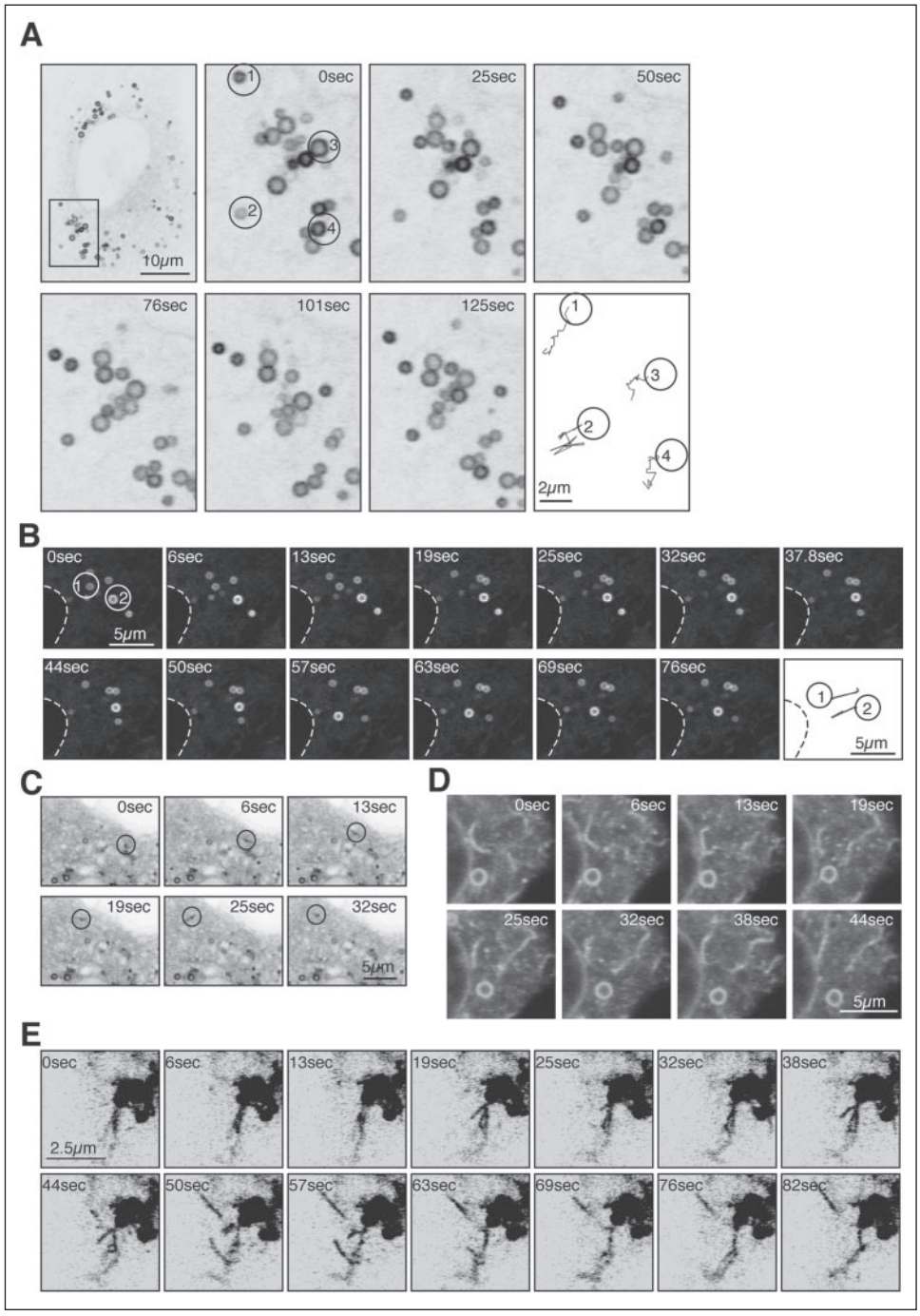

FIGURE 6. **Real-time video microscopy of GFP-Rab18 in LDs and the ER.** Vero cells expressing GFP-Rab18 were incubated overnight with 100 μg/ml oleic acid then imaged in real-time in the absence of oleic acid. The motility of GFP-Rab18 was analyzed at ~6-s intervals for a total of 3 min. *A* and *B*, GFP-Rab18-labeled LDs were observed to oscillate, in addition to undergoing saltatory motility (see supplementary data, videos 1 and 2). Tracking the motility of individual LD particles demonstrated that, although the majority of movements were small (*A1*, *A3*, and *A4*, <0.5 μm), around 6% of LD particles underwent longer (>2 μm) vectorial movements (*A2*, *B1*, and *B2*). The rate of vectorial transport was estimated to be ~1 μm/s. *C*, punctate foci of GFP-Rab18 labeling were observed to undergo rapid movements in the periphery of the cell (see supplementary data, video 3). *D* and *E*, GFP-Rab18 in the ER clearly demonstrated the dynamic nature of the ER membranes throughout the cell and toward the cell surface (*D*) (see supplementary data, videos 4 and 5). In addition, GFP-Rab18-labeled ER elements were seen to extend away from groups of LDs in the perinuclear region of the cell (*E*).

High expression of mRFP-Cav3^{DGV} relative to GFP-Rab18 prevented the localization of GFP-Rab18 to the LD surface and restricted it to the ER (results not shown). Following treatment of co-expressing cells with oleic acid LDs were predominantly labeled by mRFP-Cav3^{DGV}, whereas GFP-Rab18 was restricted to the ER and small puncta (Fig. 7*C*).

To gain further insights into the association of Rab18 with specific LD populations, we examined LD biogenesis in cells expressing GFP-Rab18 or mRFP-Cav3^{DGV}. Vero cells expressing GFP-Rab18 with or without mRFP-Cav3^{DGV} were serum-starved overnight to reduce the number of existing LDs and incubated in normal medium containing 100 μg/ml oleic acid for 0–6 h. LDs were identified by staining neutral lipids using Nile Red (with GFP-Rab18) or using Bodipy493/503 (with mRFP-Cav3^{DGV}). Nascent LDs were first detectable within 15–30 min following the addition of oleic acid and were clearly identifiable by 1 h. Following serum starvation, GFP-Rab18 was predominantly present in the ER and was first observed associating with LDs between 1 and 3 h after addition of oleic acid, suggesting exclusion from LDs during the earliest time points of biogenesis (Fig. 8*A*). In contrast, although mRFP-Cav3^{DGV} was also observed in the ER following serum starvation, it was first observed to label LDs within 15 min of initiating biogenesis (results not shown) and was clearly detectable in LDs after 1 h (Fig. 8*B*). Following co-expression of mRFP-Cav3^{DGV} and GFP-Rab18, the association of mRFP-Cav3^{DGV} with forming LDs was found to be identical to control conditions (Fig. 8*C*). However, GFP-Rab18 was unable to associate with LDs in the presence of mRFP-Cav3^{DGV} even following 6 h of formation, suggesting that the presence of mRFP-Cav3^{DGV} at the LD surface pre-

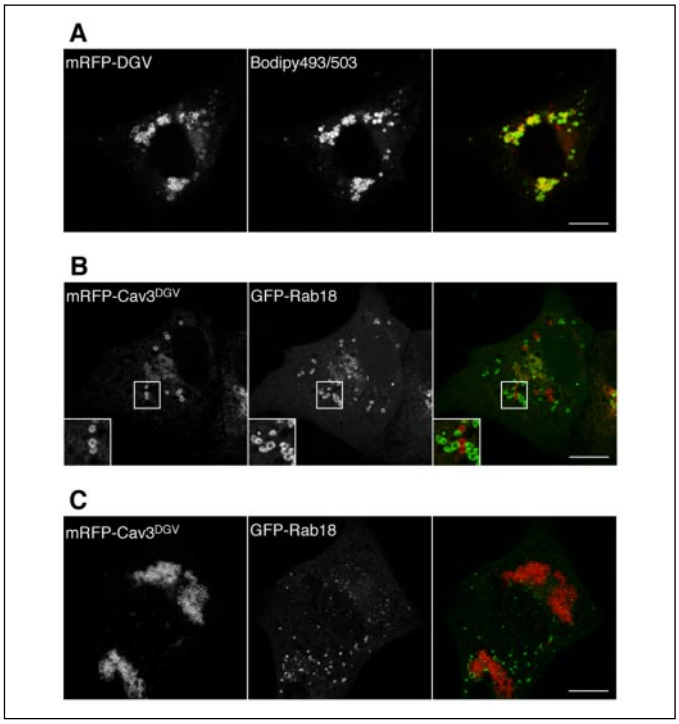

FIGURE 7. **GFP-Rab18 and mRFP-Cav3^{DGV} localize to distinct LD populations.** Vero cells were transfected with mRFP-Cav3^{DGV} in the presence or absence of GFP-Rab18 and incubated in the presence or absence of 100 μg/ml oleic acid overnight. Cells were subsequently fixed in 4% PFA and analyzed by fluorescent microscopy. *A*, in oleic acid-treated cells mRFP-Cav3^{DGV} was predominantly localized to large clusters of LDs in the perinuclear region, in addition to low labeling of the ER and in the Golgi area. *B*, in control cells mRFP-Cav3^{DGV} and GFP-Rab18 were localized to distinct LD populations following co-transfection. *C*, in co-transfected cells treated with oleic acid overnight, mRFP-Cav3^{DGV} localization was identical to that observed in the absence of GFP-Rab18. In contrast, GFP-Rab18 showed a significantly reduced LD localization and was predominantly localized to the ER, to very small LDs and to small puncta throughout the cells. *Scale bars* = 10 μm.

vents the recruitment of GFP-Rab18, either directly or indirectly, and further implying that Rab18 is not required for the biogenesis of LDs.

In conclusion, we have shown that GFP-Rab18 labels a distinct population of LDs and does not associate with LDs labeled by an inhibitory caveolin mutant. Although the caveolin mutant associates with forming "early" LDs, Rab18 associates specifically with "late" LDs. In addition, we have shown that expression of the caveolin mutant prevents the association of Rab18 with the LD surface.

Stimulation of Lipolysis in Adipocytes Causes Translocation of Rab18 to the LD Surface—We hypothesized that the association of Rab18 with distinct LDs in the same cell may reflect a particular functional state of individual LDs. Proteomic analysis of LDs from basal and lipolytically active adipocytes has identified Rab18 as a candidate LD protein only under conditions of lipolysis (11). Therefore, we examined whether the localization of Rab18 was regulated by the metabolic state of the adipocyte. Stimulation of lipolysis by catecholamines occurs via a signaling cascade from the cell surface β-adrenergic receptor through $G_{\alpha s}$ activation of adenylate cyclase, up-regulation of cAMP levels resulting in the activation of protein kinase A, and phosphorylation of two proteins involved in the regulation of lipolysis, hormone-sensitive lipase and perilipin (33). Lipolysis can be stimulated by isoproterenol activation of the β-adrenergic receptor, or by elevation of intracellular cAMP levels using forskolin to activate adenylate cyclase. In contrast, isoproterenol stimulation of lipolysis can be inhibited using propranolol, a β-adrenergic antagonist.

Following stimulation of lipolysis in 3T3-L1 adipocytes for 30 min using either 10 μM isoproterenol or 20 μM forskolin there was increased labeling of Rab18 at the surface of LDs detected by immunofluorescence microscopy (Fig. 9*A*), concomitant with the fragmentation of perilipin-labeled LDs (Ref. 34 and results not shown). In contrast, when lipolysis was stimulated using 10 μM isoproterenol for 30 min, followed by the addition of 200 μM propranolol for a further 60 min, the translocation of Rab18 to the LD was completely reversed, suggesting that the association of Rab18 with the LD is tightly associated with the metabolic state of the cell. Quantification of the average pixel intensity of Rab18 immunofluorescence at the LD surface showed a ~2-fold increase in Rab18 labeling (Fig. 9*B*) in lipolytically active cells compared with cells in normal growth medium, or cells treated with the β-adrenergic antagonist. Three-dimensional rendering of the Rab18 labeling of LDs in lipolytically active cells demonstrated that Rab18 was present over the entire surface of the LD and was found on both large and smaller LDs (Fig. 9*C*).

Biochemical isolation of LDs showed that Rab18 was associated with this organelle in control cells and that this association increased by ~6-fold following activation of lipolysis (Fig. 9, *D* and *E*). Recruitment of Rab18 to the LD fraction occurred concomitant with the slowed mobility of perilipin on SDS-PAGE, consistent with its well characterized hyperphosphorylation in lipolytically active cells (Fig. 9*E*) (33). From these experiments we conclude that Rab18 is specifically recruited to LDs in lipolytically active cells.

DISCUSSION

Although lipid droplets have been well described in specific cell types such as adipocytes and steroidogenic cells, in recent years it has become clear that a vast variety of cell types have the capacity to synthesize neutral lipids and generate LDs in a regulated and dynamic manner (1). Despite these advances and the obvious importance of understanding the regulation of LD function for diseases such as obesity and diabetes, the molecular mechanisms underlying LD biogenesis, motility, and catabolism are still poorly understood. In the present study we have identified a member of the Rab family of small GTPases, Rab18, which shows a regulated association with the monolayer of the LD.

Rab proteins have been shown to play a leading role as membrane organizers, integrating membrane tethering and fusion with cytoskeleton-dependent motility, through their association with multiple effector proteins (15, 16). Proteomic analyses have identified over 10 different Rab proteins associated with LDs across a range of cell types (11–14). Although it is likely that a number of the Rab proteins identified in LDs are involved in the regulation of LD function, the close physical association shown in this study between LDs and both endosomal compartments and the ER suggests that, in the absence of independent evidence for a direct role, the possibility of contamination of LD preparations with membrane proteins derived from other compartments cannot be overlooked. Further independent analyses of other putative LD Rab proteins will need to be undertaken before a clear picture can emerge of the range and importance of LD interactions with other membrane compartments.

Rab18: A Lipid Droplet-associated Rab Protein—In the present study we have used light microscopy, immunoelectron microscopy, and biochemistry to localize epitope-tagged, heterologously expressed Rab18 to the LD surface. In addition, localization to LDs was confirmed using antibodies raised against the endogenous Rab18 protein. These studies clearly demonstrate that Rab18 associates with a specific subset of LDs in both the 3T3-L1 adipocyte model system and in the non-adipocyte cell lines tested. Our previous Northern blot analyses (18) showed that Rab18 has a ubiquitous expression pattern in mammalian tissues, with particularly high expression in epithelia and brain. In kidney epithelial cells, Rab18 was localized to smooth tubular membranes close to the

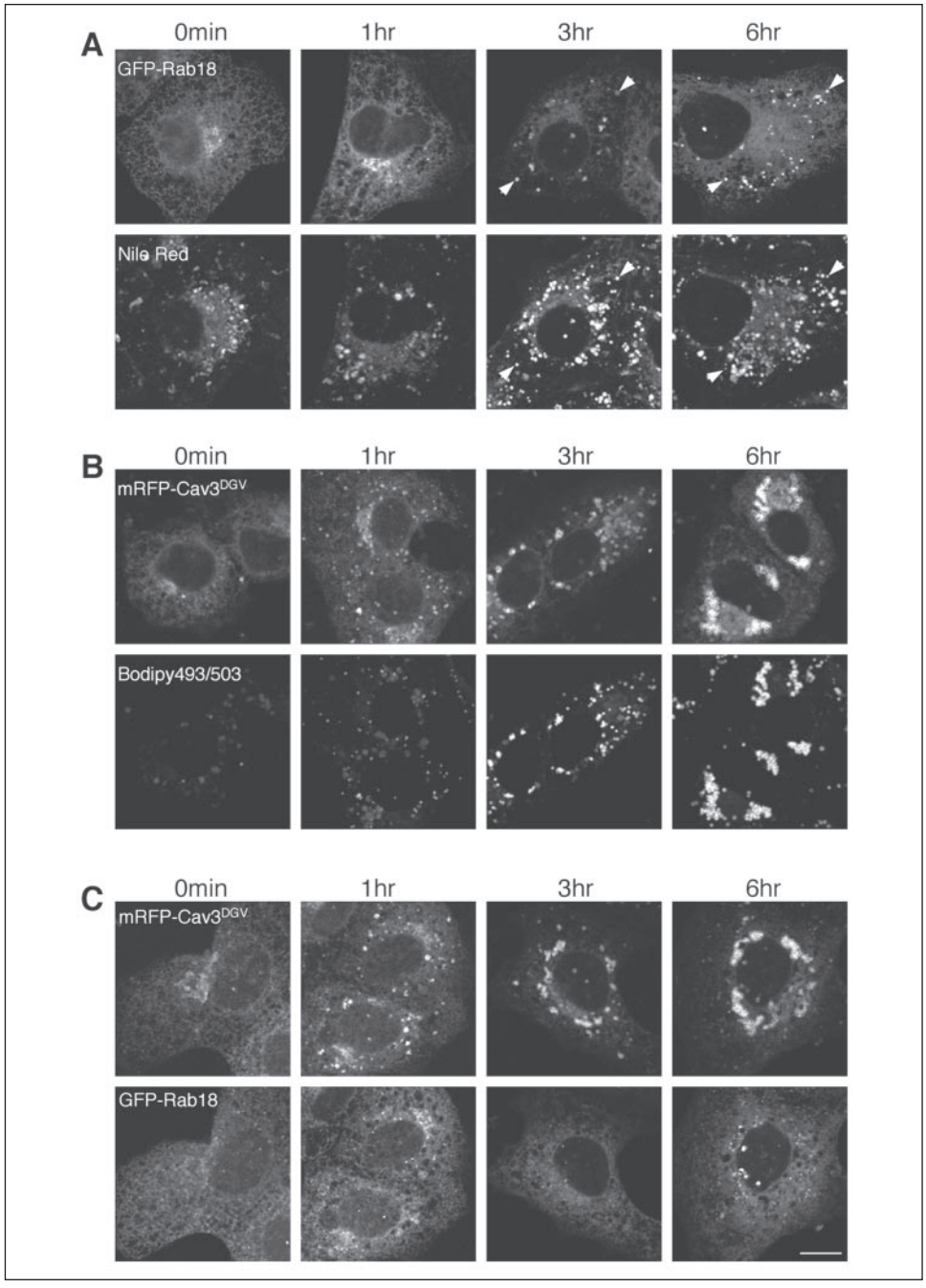

FIGURE 8. **mRFP-Cav3^{DGV} localization to forming LDs precedes that of GFP-Rab18.** Vero cells were transfected with GFP-Rab18 and mRFP-Cav3^{DGV} either separately or in combination, then incubated in serum-free medium overnight to reduce the number of existing LDs. Cells were subsequently incubated in 100 μg/ml oleic acid for 0–6 h prior to fixation in 4% PFA. *A*, cells expressing GFP-Rab18 were counterstained using Nile Red to label LDs. There was no detectable labeling of forming LDs at 1 h, but significant labeling of a subset of LDs was detected at 3 h (*arrows*). *B*, cells expressing mRFP-Cav3^{DGV} were counterstained using Bodipy493/503 to label LDs. The localization of mRFP-Cav3^{DGV} to forming LDs was detectable within 1 h. *C*, in cells co-expressing both mRFP-Cav3^{DGV} and GFP-Rab18, localization of mRFP-Cav3^{DGV} to the LD surface was detected within 1 h. In contrast, GFP-Rab18 showed little LD localization during the period of the time course. *Scale bar* = 10 μm.

apical cell surface, proposed to be endosomal compartments based on ultrastructural analyses, and was also localized to Rab5-labeled structures upon overexpression as judged by light microscopy (18). In the present study we failed to identify GFP-Rab18 in endosomal structures by light microscopy and the punctate labeling observed for endogenous Rab18 did not coincide with expressed GFP-Rab5.[3] However, as shown here, endosomal structures can closely appose (Fig. 1), and even partially enwrap,[3] LDs. However, before endosomal localization is dismissed more detailed analysis of Rab18 localization in different tissues is clearly required. Localization of Rab18 to LDs and ER is at least consistent with phylogenetic analysis of mammalian Rab GTPases, in which Rab18 is more closely related to Rab proteins involved in ER and Golgi trafficking processes, than in endosomal traffic (35).

Rab18 Localizes to the Monolayer Surface of a Subset of LDs—In the present study we have identified GFP-Rab18 at the LD surface and confirmed by electron microscopy that this represents association with the monolayer of the LD. LD localization was seen over a wide range of expression levels and was confirmed by labeling for the endogenous Rab18 protein. Intriguingly, even in cells expressing high levels of Rab18 not all LDs are labeled, and those that are labeled can have extremely high levels of Rab18. This raises interesting questions about the mechanisms involved in targeting Rab18 to the surface of these particular LDs and the molecular determinants dictating Rab18 recruitment to specific LD populations. Analysis of the effectors and other interacting proteins for some of the best understood Rabs have shown that an individual Rab

[3] S. Martin and R. Parton, unpublished data.

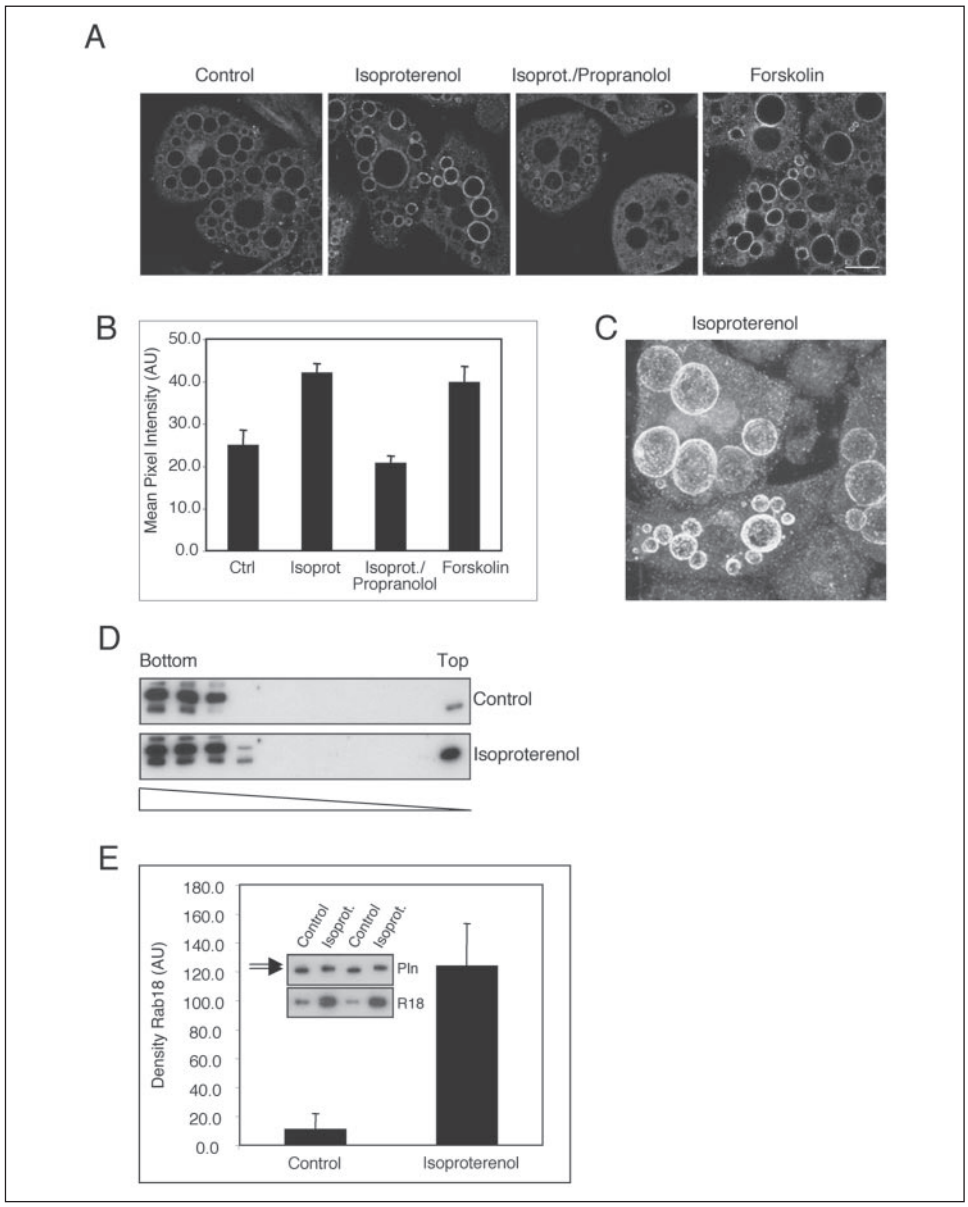

FIGURE 9. **Rab18 localization to LDs is increased following stimulation of lipolysis.** *A*, 3T3-L1 adipocytes were either fixed directly (control), or incubated with 10 μM isoproterenol for 30min (*Isoproterenol*), 10 μM isoproterenol for 30 min followed by 200 μM propranolol for 60 min (*Isoprot./Propranolol*) or 20 μM forskolin for 30 min, prior to fixation. Cells were subsequently labeled for Rab18. *Scale bar* = 10 μM. *B*, the mean pixel intensity of Rab18 labeling at the LD surface was determined as described under "Materials and Methods" (n = 2, results ± S.D.). Immunofluorescence labeling of Rab18 at the surface of the LDs was found to increase dramatically following stimulation of lipolysis. *C*, three-dimensional rendering of the Rab18 labeling in isoproterenol-treated cells demonstrated that Rab18 labeled patches over the entire surface of both small and large LDs. *D*, 3T3-L1 adipocytes were incubated with or without 10 μM isoproterenol for 30 min prior to the preparation of cell lysates and fractionation of LDs using a sucrose density gradient. Gradients were analyzed by Western blotting for Rab18. *E*, LD fractions from the top of the sucrose density gradients were analyzed by Western blotting for Rab18 (*R18*) and Perilipin (*Pln*). Treatment with isoproterenol resulted in an increased association of Rab18 with the LD fraction, concomitant with altered mobility of perilipin, consistent with its phosphorylation. Rab18 in the LD fraction was quantified by densitometry (n = 4, results ± S.D.).

can be associated with >30 distinct proteins, either directly or indirectly (16). Furthermore, the attachment of Rab proteins to a particular membrane can be mediated not only by protein factors but also by specific phospholipids present in a domain of the membrane. To date, no interacting proteins or lipids have been identified for Rab18.

In addition to labeling of the LD monolayer, we also observed association of heterologously expressed Rab18 with the ER and with discrete clusters of tubulovesicular elements the nature of which has not yet been identified. We hypothesize that these correspond to the rapidly moving punctate structures identified by real-time microscopy. Although ER labeling was not consistently seen with antibodies against the endogenous protein, ER and TVE labeling was very specific when compared with other cellular membranes, and we assume that the lower level of Rab18 in the ER is below the detection of the antibodies. Rab18 is unusual in the Rab family in that the extreme C terminus contains a mono-cysteine prenylation motif rather than the di-cysteine prenylation motifs present in most other Rab family members. Although the reason for this difference is not known, it could be that mono-prenylation is required for Rab18 to associate with the LD monolayer. Previous studies have shown that mutation of di-cysteine prenylation sites in endosomal Rabs to mono-cysteines results in their mis-localization to the ER (36–38), suggesting the possibility that targeting of GFP-Rab18 to the ER observed in this study could result from the default insertion of a naturally occurring mono-cysteine Rab into the ER in the absence of sufficient numbers of LDs. However, we consider this unlikely to be the case, because, under all experimental conditions used in this study, for both catabolism and LD formation, only a subset of LDs were ever labeled for Rab18 while labeling of the ER was consistently observed. The importance of Rab18 ER targeting and its relationship to lipolysis and LD function are not yet known.

Regulation of Rab18 Recruitment to LDs in Adipocytes upon Lipolysis—In this study we have directly demonstrated recruitment of a Rab protein to LDs in adipocytes in response to lipolytic stimulation. In view of the importance of understanding lipid regulation in the adipocyte to obesity this is a very significant finding. Stimulation of lipolysis in adipocytes has been well characterized (33). The mechanism of Rab18 recruitment is not yet known, but interestingly in control cells the majority of Rab18 was membrane-associated, suggesting that stimulation of lipolysis does not induce direct

recruitment of a cytosolic pool. It will be of fundamental importance to determine whether stimulation of lipolysis in an adipocyte cell line, where lipolysis is regulated through a cell type-specific mechanism, recruits a similar set of Rab18 effectors to lipolysis in non-adipocyte cell lines.

Rab18 and a Caveolin Mutant Label Distinct LD Populations, Which Differ in Metabolic State and Motility—We have previously demonstrated that a caveolin truncation mutant ($Cav3^{DGV}$) shows constitutive association with LDs (3), perturbs cellular cholesterol balance, inhibits signaling at the cell surface (39), causes neutral lipid accumulation due to inhibition of LD catabolism (8), and completely blocks LD motility. The primary molecular mechanisms underlying the effects of $Cav3^{DGV}$ expression are not yet clear. A striking finding of the present study was the mutually exclusive association of $Cav3^{DGV}$ and Rab18 with LDs. Studies of LD biogenesis illuminated clear differences in the association of Rab18 and $Cav3^{DGV}$. $Cav3^{DGV}$ associates with the very earliest LDs detectable after oleic acid addition, whereas Rab18 associates with presumably fully formed LDs at much later times. This suggests that $Cav3^{DGV}$ and Rab18 define functionally distinct LD populations. The surface properties of forming LDs are clearly different from those of later LDs. At high expression levels $Cav3^{DGV}$ completely inhibits Rab18 recruitment to LDs. Together with our previous studies our results suggest that inhibition of LD motility by the caveolin mutant has functional consequences on LDs, both in terms of catabolism and maintenance of surface free cholesterol levels but also at the molecular level as judged by Rab18 recruitment. Although we have no evidence to suggest that the primary effect of $Cav3^{DGV}$ is to inhibit Rab18 recruitment, we cannot rule this out.

An intriguing model is that Rab18 regulates motility required for lipid distribution to cellular membranes. LDs have been observed in apposition to many intracellular organelles, including both endosomes and the ER. It is possible that direct apposition of LDs to the limiting membranes of other organelles can facilitate the direct redistribution of lipids in response to cellular requirements. During submission of this analysis, a study describing association of Rab18 with LDs in hepatocytes was published, and a role in ER recruitment around LDs was proposed (40). In a series of experiments undertaken using both dominant-negative mutants of Rab18 and Rab18 siRNA, we have been unable to definitively identify changes in LD formation or catabolism (results not shown). We believe that this reflects the complexity of LD regulation and/or function, of which very little is currently known, as well as the fact that Rab18 associates with a distinct lipid droplet population and consequently we may not see an effect on the entire LD population. However, the characterization of a Rab protein associated with LDs provides an important new system to understand machinery involved in LD function and the role of this fascinating organelle in cellular function.

Acknowledgments—We thank Prof. John Hancock for the provision of antibodies, Prof. Roger Tsien for providing the pRSET-mRFP construct, Dr. Lucas Pelkmans for providing the pEGFP-Rab7 construct, and Dr. Richard Newton for the gift of forskolin. We also thank Annika Stark and Samantha Murphy for technical assistance, Matthew Kirkham for critical reading of the manuscript, and John Presley for discussion of his observations prior to publication.

REFERENCES

1. Martin, S., and Parton, R. G. (2005) *Semin. Cell Dev. Biol.* **16,** 163–174
2. Murphy, D. J. (2001) *Prog. Lipid Res.* **40,** 325–438
3. Pol, A., Martin, S., Fernandez, M. A., Ferguson, C., Carozzi, A., Luetterforst, R., Enrich, C., and Parton, R. G. (2004) *Mol. Biol. Cell* **15,** 99–110
4. Targett-Adams, P., Chambers, D., Gledhill, S., Hope, R. G., Coy, J. F., Girod, A., and McLauchlan, J. (2003) *J. Biol. Chem.* **278,** 15998–16007
5. Valetti, C., Wetzel, D. M., Schrader, M., Hasbani, M. J., Gill, S. R., Kreis, T. E., and Schroer, T. A. (1999) *Mol. Biol. Cell* **10,** 4107–4120
6. Blanchette-Mackie, E. J., Dwyer, N. K., Barber, T., Coxey, R. A., Takeda, T., Rondinone, C. M., Theodorakis, J. L., Greenberg, A. S., and Londos, C. (1995) *J. Lipid Res.* **36,** 1211–1226
7. Vock, R., Hoppeler, H., Claassen, H., Wu, D. X., Billeter, R., Weber, J. M., Taylor, C. R., and Weibel, E. R. (1996) *J. Exp. Biol.* **199,** 1689–1697
8. Pol, A., Luetterforst, R., Lindsay, M., Heino, S., Ikonen, E., and Parton, R. G. (2001) *J. Cell Biol.* **152,** 1057–1070
9. Murata, M., Peranen, J., Schreiner, R., Wieland, F., Kurzchalia, T. V., and Simons, K. (1995) *Proc. Natl. Acad. Sci. U. S. A.* **92,** 10339–10343
10. Trigatti, B. L., Anderson, R. G., and Gerber, G. E. (1999) *Biochem. Biophys. Res. Commun.* **255,** 34–39
11. Brasaemle, D. L., Dolios, G., Shapiro, L., and Wang, R. (2004) *J. Biol. Chem.* **279,** 46835–46842
12. Liu, P., Ying, Y., Zhao, Y., Mundy, D. I., Zhu, M., and Anderson, R. G. (2004) *J. Biol. Chem.* **279,** 3787–3792
13. Fujimoto, Y., Itabe, H., Sakai, J., Makita, M., Noda, J., Mori, M., Higashi, Y., Kojima, S., and Takano, T. (2004) *Biochim. Biophys. Acta* **1644,** 47–59
14. Umlauf, E., Csaszar, E., Moertelmaier, M., Schuetz, G. J., Parton, R. G., and Prohaska, R. (2004) *J. Biol. Chem.* **279,** 23699–23709
15. Seabra, M. C., and Wasmeier, C. (2004) *Curr. Opin. Cell Biol.* **16,** 451–457
16. Zerial, M., and McBride, H. (2001) *Nat. Rev. Mol. Cell Biol.* **2,** 107–117
17. Shewan, A. M., Marsh, B. J., Melvin, D. R., Martin, S., Gould, G. W., and James, D. E. (2000) *Biochem. J.* **350,** 99–107
18. Lutcke, A., Parton, R. G., Murphy, C., Olkkonen, V. M., Dupree, P., Valencia, A., Simons, K., and Zerial, M. (1994) *J. Cell Sci.* **107,** 3437–3448
19. Prior, I. A., Harding, A., Yan, J., Sluimer, J., Parton, R. G., and Hancock, J. F. (2001) *Nat. Cell Biol.* **3,** 368–375
20. Sonnichsen, B., De Renzis, S., Nielsen, E., Rietdorf, J., and Zerial, M. (2000) *J. Cell Biol.* **149,** 901–914
21. Luetterforst, R., Stang, E., Zorzi, N., Carozzi, A., Way, M., and Parton, R. G. (1999) *J. Cell Biol.* **145,** 1443–1459
22. Campbell, R. E., Tour, O., Palmer, A. E., Steinbach, P. A., Baird, G. S., Zacharias, D. A., and Tsien, R. Y. (2002) *Proc. Natl. Acad. Sci. U. S. A.* **99,** 7877–7882
23. Yu, W., Cassara, J., and Weller, P. F. (2000) *Blood* **95,** 1078–1085
24. Morrow, I. C., Rea, S., Martin, S., Prior, I. A., Prohaska, R., Hancock, J. F., James, D. E., and Parton, R. G. (2002) *J. Biol. Chem.* **277,** 48834–48841
25. Martin, S., Tellam, J., Livingstone, C., Slot, J. W., Gould, G. W., and James, D. E. (1996) *J. Cell Biol.* **134,** 625–635
26. Martin, S., Ramm, G., Lyttle, C. T., Meerloo, T., Stoorvogel, W., and James, D. E. (2000) *Traffic* **1,** 652–660
27. Martin, S., Rice, J. E., Gould, G. W., Keller, S. R., Slot, J. W., and James, D. E. (1997) *J. Cell Sci.* **110,** 2281–2291
28. Tokuyasu, K. T. (1980) *Histochem. J.* **12,** 381–403
29. Liou, W., Geuze, H. J., and Slot, J. W. (1996) *Histochem. Cell Biol.* **106,** 41–58
30. Bucci, C., Thomsen, P., Nicoziani, P., McCarthy, J., and van Deurs, B. (2000) *Mol. Biol. Cell* **11,** 467–480
31. Chavrier, P., Parton, R. G., Hauri, H. P., Simons, K., and Zerial, M. (1990) *Cell* **62,** 317–329
32. Roberts, R. L., Barbieri, M. A., Pryse, K. M., Chua, M., Morisaki, J. H., and Stahl, P. D. (1999) *J. Cell Sci.* **112,** 3667–3675
33. Tansey, J. T., Sztalryd, C., Hlavin, E. M., Kimmel, A. R., and Londos, C. (2004) *IUBMB Life* **56,** 379–385
34. Londos, C., Brasaemle, D. L., Schultz, C. J., Adler-Wailes, D. C., Levin, D. M., Kimmel, A. R., and Rondinone, C. M. (1999) *Ann. N. Y. Acad. Sci.* **892,** 155–168
35. Pereira-Leal, J. B., and Seabra, M. C. (2000) *J. Mol. Biol.* **301,** 1077–1087
36. Calero, M., Chen, C. Z., Zhu, W., Winand, N., Havas, K. A., Gilbert, P. M., Burd, C. G., and Collins, R. N. (2003) *Mol. Biol. Cell* **14,** 1852–1867
37. Gomes, A. Q., Ali, B. R., Ramalho, J. S., Godfrey, R. F., Barral, D. C., Hume, A. N., and Seabra, M. C. (2003) *Mol. Biol. Cell* **14,** 1882–1899
38. Overmeyer, J. H., Wilson, A. L., and Maltese, W. A. (2001) *J. Biol. Chem.* **276,** 20379–20386
39. Roy, S., Luetterforst, R., Harding, A., Apolloni, A., Etheridge, M., Stang, E., Rolls, B., Hancock, J. F., and Parton, R. G. (1999) *Nat Cell Biol.* **1,** 98–105
40. Ozeki, S., Cheng, J., Tauchi-Sato, K., Hatano, N., Taniguchi, H., and Fujimoto, T. (2005) *J. Cell Sci.* **118,** 2601–2611

Regulated Localization of Rab18 to Lipid Droplets: EFFECTS OF LIPOLYTIC STIMULATION AND INHIBITION OF LIPID DROPLET CATABOLISM

Sally Martin, Kim Driessen, Susan J. Nixon, Marino Zerial and Robert G. Parton

J. Biol. Chem. 2005, 280:42325-42335.
doi: 10.1074/jbc.M506651200 originally published online October 5, 2005